

# Quench dynamics of a disordered array of dissipative coupled cavities

C. Creatore,<sup>1</sup> R. Fazio,<sup>2</sup> J. Keeling,<sup>3</sup> and H. E. Türeci<sup>4</sup>

<sup>1</sup>*Cavendish Laboratory, University of Cambridge, CB3 0HE Cambridge, United Kingdom*

<sup>2</sup>*NEST, Scuola Normale Superiore and Istituto Nanoscienze-CNR, I-56127 Pisa, Italy*

<sup>3</sup>*Scottish Universities Physics Alliance, School of Physics and Astronomy,  
University of St Andrews, St Andrews KY16 9SS, United Kingdom*

<sup>4</sup>*Department of Electrical Engineering, Princeton University, Princeton, New Jersey 08544, USA*

We investigate the mean-field dynamics of a system of interacting photons in an array of coupled cavities in presence of dissipation and disorder. We follow the evolution of an initially prepared Fock state, and show how the interplay between dissipation and disorder affects the coherence properties of the cavity emission and that these properties can be used as signatures of the many-body phase of the whole array.

## I. INTRODUCTION

The idea of understanding the behaviour of complex quantum many-body systems using experimentally controllable *quantum simulators* can be traced back to a pioneering keynote speech given by Richard Feynman in 1982<sup>1</sup>. After thirty years, quantum simulation is now a thriving field of research<sup>2,3</sup>, driven by the increasing ability to design and fabricate controllable quantum systems, in contexts ranging from superconducting-circuits<sup>4</sup> to ultracold atoms<sup>5</sup> or trapped ions<sup>6</sup>. These systems allow the realisation of archetypal models and the exploration of new physical regimes. An area of recently developing interest has been coupled cavity arrays, lattices of coupled matter-light systems, providing highly tunable but dissipative quantum systems<sup>7–11</sup>.

Physical realisations of coupled cavity arrays have been proposed in a variety of systems, such as photonic crystal nanocavities<sup>12</sup>, coupled optical waveguides<sup>13</sup>, or lattices of superconducting resonators operating in the microwave regime<sup>4,14,15</sup>. While experiments have not yet probed the collective behaviour predicted in large scale arrays, progress towards such realisations is very encouraging. For these different systems, the radiation modes involved range from microwave to optical frequency; we will nonetheless refer to these as coupled “matter-light” systems in the following, taking “light” to refer to the radiation modes.

A generic coupled cavity array (CCA) consists of a lattice of cavities, each supporting a confined photon quasi-mode. We refer to quasi-modes<sup>16</sup> since the finite quality of the cavities implies there will be coupling to the outside world. As shown in Fig. 1, the cavities are coupled through photon hopping. A purely optical system would be entirely linear, and thus unable to simulate interacting many-body quantum systems. To introduce nonlinearity requires coupling to matter (e.g. suitable optical emitters such as semiconductor quantum dots or superconducting qubits, indicated by blue circles in Fig. 1). This leads to a system of photons hopping on a lattice, with an on-site nonlinearity and on-site losses.

A wide variety of different microscopic models can be realised depending on the precise design of the ar-

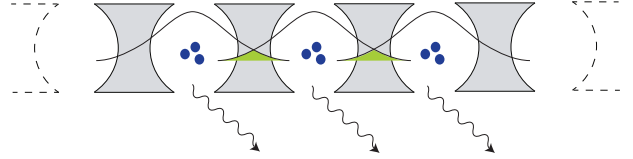


FIG. 1. A sketch of a one-dimensional cavity array as described in the text.

ray<sup>10,11,15</sup>. We consider here the archetypal case where the CCA can be mapped<sup>10</sup> onto the Bose-Hubbard model<sup>17</sup>. This corresponds to the regime of weak matter-light coupling, i.e. strong detuning between cavity mode and matter degrees of freedom<sup>18</sup>.

In the absence of dissipation, the ground state phase diagram of the Bose-Hubbard model has been extensively studied<sup>5</sup>: At zero temperature a quantum phase transition results from the competition between on-site nonlinearities and inter-site photon hopping. When the nonlinearities are strong and prevail over the hopping, the photons are localised by interactions, leading to an insulating Mott phase; in the opposite regime, when photon hopping dominates, a superfluid phase characterised by long-range coherence occurs. Coupled matter-light systems however are naturally studied under non-equilibrium conditions, as there are invariably photon losses. As such, a steady state in a coupled cavity array requires external pumping. The steady-state of cavity arrays, resulting from the competition of external driving and dissipation, has been the subject of much recent theoretical interest<sup>18–23</sup>.

Besides the steady state, the transient dynamics of cavity arrays may bring additional interesting information. By engineering suitable laser pulse sequences<sup>24,25</sup> it is possible to prepare a specific initial state and follow its subsequent evolution by analysing the properties of the light escaping from the system. This is the situation considered in [26], considering the evolution following preparation of a Fock state. Such a protocol is equivalent to studying a quantum quench in an open system. Quantum quenches in closed systems are an intensively studied paradigm of non-equilibrium dynamics of many-body systems<sup>27</sup>, and in the closed Bose-Hubbard model

have been already addressed both theoretically and experimentally, see [27–30]. Cavity arrays appear to be ideally suited to explore the transient dynamics following a quench.

Remarkably, even in the lossy system, the dynamics following such a quench clearly map out a superfluid–insulator transition<sup>26</sup>. In fact, in mean-field theory these can be directly related to the equilibrium phase boundary<sup>26,31</sup>. In particular, by rescaling correlation functions by the decaying density one finds that the behaviour at long times is distinct for values of hopping in the superfluid and insulating phases — the rescaled coherence vanishes in the insulating phase, but attains a non-zero asymptote in the superfluid phase. As discussed further below, this can be traced back to the way in which for the closed system quench, the linear stability of an initial Mott state reproduces the equilibrium phase diagram<sup>32</sup>. Given the notable ability of the rescaled correlations of the open system to reproduce the equilibrium phase boundary, and the significant interest in the disordered Bose-Hubbard model<sup>17,33–35</sup>, a natural question to ask is how the open system quench dynamics are affected by disorder. This is the question we being to address in this paper. Building on the results of Tomadin *et al.*<sup>26</sup>, we analyse the non-equilibrium mean-field dynamics of an array of non-linear coupled cavities in presence of photon leakage and disorder in the on-site cavity energies.

The paper is organised as follows: In Section 2 we introduce the model used to describe the dissipative and disordered cavity array; in Section 3 we analyse the dynamics of the correlation functions of the cavity array, first summarising the results for the ideal *clean case* and then assuming a Gaussian distribution for the on-site cavity energies, and compare the results; in Section 4 we briefly discuss an anomalous behaviour of the second order correlation function in presence of disorder; in Section 5 we summarise our conclusions.

## II. MODEL SYSTEM AND INITIAL STATE

As discussed above, we consider the Bose-Hubbard model<sup>17</sup> described by the Hamiltonian:

$$\hat{H} = \sum_i \frac{U}{2} \hat{n}_i(\hat{n}_i - 1) + \varepsilon_i \hat{n}_i - J \sum_{\langle ij \rangle} \hat{b}_i^\dagger \hat{b}_j. \quad (1)$$

Here  $\hat{b}_i^\dagger$  ( $\hat{b}_i$ ) creates (annihilates) a photon in the  $i$ -th site and the corresponding number operator is  $\hat{n}_i = \hat{b}_i^\dagger \hat{b}_i$ . The energy of the photon mode in the  $i$ th cavity is  $\varepsilon_i$ ,  $J$  denotes the amplitude for inter-site photon hopping, while  $U$  represents the on-site nonlinearity resulting from the coupling to matter. Including also the presence of Markovian photon loss leads to the master equation:

$$\partial_t \rho(t) = -i[\hat{H}, \rho(t)] + \kappa \sum_i \mathcal{D}[\hat{b}_i, \rho], \quad (2)$$

where loss is described by the Lindblad term  $\mathcal{D}[X, \rho] = 2X\rho X^\dagger - X^\dagger X\rho - \rho X^\dagger X$ . The photon lifetime is  $(2\kappa)^{-1}$ . We consider the case where  $U, \kappa, J$  are independent of site, but there may be disorder in the energies  $\varepsilon_i$ . We will discuss below the “clean” case in which all  $\varepsilon_i$  are the same, and the disordered case where we will choose cavity energies  $\varepsilon_i$  to be drawn from Gaussian distribution having mean value  $\bar{\varepsilon} = \varepsilon_0$  and variance  $\sigma^2$ , with  $\sigma$  representing the strength of the disorder. The mean value  $\bar{\varepsilon}$  can be removed by a gauge transformation, and so may be set to zero without loss of generality. The numerical integration of the master equation has been implemented using a fourth- and fifth-order Runge-Kutta algorithm and we truncate the Fock basis for each cavity to  $\{|n\rangle_i\}_{n=0}^{n_{\max}}$  with  $n_{\max} = 4$ .

We explore the quench dynamics of this model in the mean-field approximation  $\rho = \prod_i \rho_i$ , which decouples the photon hopping between neighbouring cavities but allows for a spatially inhomogeneous solution. Such an approximation is expected to be valid in the limit of large coordination  $z$ , where  $z$  is the number of nearest neighbours of each site. The dynamics of each cavity is governed by the master equation

$$\partial_t \rho_i(t) = \mathcal{L} \rho_i(t), \quad (3)$$

$$\mathcal{L} = -i[\hat{h}_i, \rho_i(t)] + \kappa \mathcal{D}[\hat{b}_i, \rho_i(t)], \quad (4)$$

$$\hat{h}_i = \frac{U}{2} \hat{n}_i(\hat{n}_i - 1) + \varepsilon_i \hat{n}_i - J(\phi_i(t) \hat{b}_i^\dagger + \phi_i^*(t) \hat{b}_i), \quad (5)$$

where  $\phi_i(t) = \sum_{j \in \text{nn}(i)} \text{Tr}[\hat{b}_j \rho_j(t)]$  is summed over the  $z$  nearest neighbours of site  $i$ . In the clean case all sites are equivalent and so  $\phi_i(t) = z \text{Tr}[\hat{b}_i \rho_i(t)]$ , and the dimensionality only enters via this factor  $z$ . In the disordered case, each site evolves separately, and the connectivity of the lattice does affect the dynamics.

Our goal in the following discussion is to study the non-equilibrium dynamics following preparation of the cavity array in a product of Fock states, i.e.  $\rho(0) = \prod_i \rho_i(0)$ ,  $\rho_i(0) = |n_0\rangle\langle n_0|$ . Because  $\text{Tr}[\hat{b}_i \rho_i(0)] = 0$  is a fixed point of the mean field equations, we consider a small deviation away from such a Fock state, and instead consider  $\rho_i(0) = |\Psi_0\rangle\langle\Psi_0|$ , where  $|\Psi_0\rangle = \sqrt{1-\eta^2}|n_0\rangle + \eta|n_0-1\rangle$ . As discussed below, depending on the parameters, the Fock state may be either a stable or unstable fixed point, and if unstable, a small initial perturbation  $\eta \ll 1$  will grow, and drive the array to a different asymptotic state.

## III. DYNAMICS OF CORRELATION FUNCTIONS

### A. Clean case

Before exploring the role played by disorder, we first summarise the results of the clean case<sup>26</sup> and present also a discussion of the initial instability, first considered

in [31] and here thoroughly discussed. In the absence of dissipation, it was shown<sup>32</sup> that when  $zJ/U > zJ/U|_{\text{cr}}$ , where  $zJ/U|_{\text{cr}}$  is the critical value corresponding to the equilibrium superfluid–insulator phase transition, an initial Fock state is linearly unstable. As such, the existence of this instability can be used to trace the equilibrium transition between the Mott and the superfluid phase<sup>31,32</sup>

$$M = \begin{pmatrix} iU(n_0 - 1) + izJn_0 - \kappa(2n_0 - 1) & (izJ + 2\kappa)\sqrt{n_0(n_0 + 1)} \\ -izJ\sqrt{n_0(n_0 + 1)} & iUn_0 - izJ(n_0 + 1) - \kappa(2n_0 + 1) \end{pmatrix}. \quad (6)$$

Instability occurs when the real part of the eigenvalues of  $M$  become positive, as this corresponds to exponential growth of fluctuations. In the absence of dissipation ( $\kappa = 0$ ), the eigenvalues  $\xi$  are given by:

$$\xi = iU \left( n_0 - \frac{1}{2} \right) - \frac{izJ}{2} \pm i\sqrt{4n_0zJU - (U - zJ)^2} \quad (7)$$

The stability boundary is at the point where the eigenvalues are both pure imaginary, and writing  $\xi = i\mu$ , one may show that  $\text{Det}(i\mu\mathbb{1} - M) = 0$  is equivalent to:

$$\frac{1}{zJ} = \frac{n_0}{\mu - U(n_0 - 1)} - \frac{n_0 + 1}{\mu - Un_0} \quad (8)$$

which is the equilibrium phase boundary for the  $n_0$ th Mott lobe. As  $zJ$  increases, the critical values of  $\mu$  in the equilibrium phase boundary approach each other, and at large enough  $zJ$ , there is no longer any real value  $\mu$  that can satisfy the above equation. As such, the instability of the Fock state corresponds to the locations of the tips of the equilibrium Mott lobes,  $zJ/U|_{\text{cr}} = (\sqrt{n_0 + 1} - \sqrt{n_0})^2$ . A comprehensive discussion of the phase boundary at finite  $\kappa$  can be found in [31]. Further, this analysis allows one to study how  $zJ/U|_{\text{cr}}$  changes when the initial state is a statistical admixture, e.g. when  $\rho(0) = \alpha^2|n_0\rangle\langle n_0| + \beta^2|n_0 + 1\rangle\langle n_0 + 1|$  ( $\alpha^2 + \beta^2 = 1$ ). In this case, for  $\kappa = 0$ , the eigenvalues  $\xi$  are given by the solutions of:

$$\frac{1}{zJ} = -\frac{i\alpha^2 n_0}{\xi + iU(n_0 - 1)} + \frac{i(\alpha^2 - \beta^2)(n_0 + 1)}{\xi + iUn_0} + \frac{i\beta^2(n_0 + 2)}{\xi + iU(n_0 + 1)}. \quad (9)$$

We note that the ground state for any incommensurate filling would always be a superfluid phase. As such, in the equilibrium phase diagram, the critical hopping jumps discontinuously as one varies the filling. Equation (9) describes a different question however; namely whether the critical hopping for a *linear* instability of the normal state evolves continuously. This is answered by Fig. 2, showing that the critical hopping  $zJ/U|_{\text{cr}}$  for this instability [obtained solving Eq. (9) for different  $n_0$ ] does

and, within our mean-field analysis, a transition survives also in the presence of dissipation.

To see this instability for the clean case, one may write coupled equations for  $\rho_{n_0-1, n_0}, \rho_{n_0, n_0+1}$  (where  $n_0$  is the occupation of the initial state, under the approximation  $\rho_{n_0, n_0} \simeq 1$ , and that all other elements of  $\rho$  are negligible). Denoting  $X = (\rho_{n_0-1, n_0}, \rho_{n_0, n_0+1})^T$ , one finds that  $X$  obeys the equation  $\partial_t X = MX$  with

evolve continuously as a function of  $\beta^2$ . In the remainder of this manuscript we restrict to the case  $\beta = 0$ .

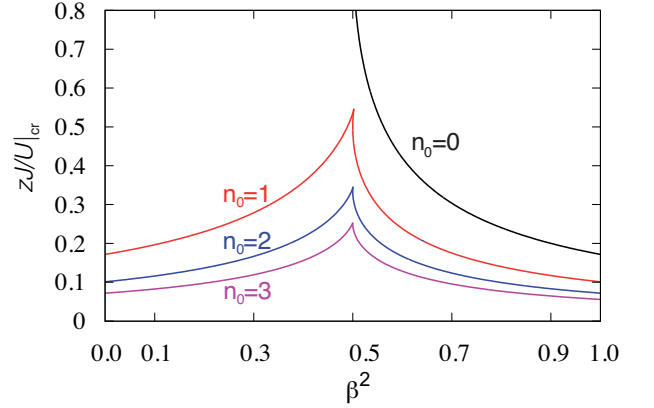


FIG. 2.  $zJ/U|_{\text{cr}}$  as a function of  $\beta^2$ , the initial state being the statistical admixture  $\rho(0) = \alpha^2|n_0\rangle\langle n_0| + \beta^2|n_0 + 1\rangle\langle n_0 + 1|$ , with  $\alpha^2 + \beta^2 = 1$ .

The consequence of this instability can be seen in the time evolution of the coherence  $\psi(t) = \text{Tr}[\hat{b}_i \rho_i(t)]$ . Figure 3 shows the evolution of  $\psi_i(t)$  for a clean system with  $zJ/U > zJ/U|_{\text{cr}}$ . The figure is plotted for parameters  $\kappa = 10^{-2}U$  and  $zJ = 0.3U$ , with an initial state with  $n_0 = 1, \eta = 10^{-5}$  — we consider this same initial state throughout the remainder of the manuscript. In the initial time range  $t\kappa \lesssim 0.1$ , due to the instability,  $\psi(t)$  grows exponentially even though the photon population  $n(t) = \text{Tr}[\hat{n}_i \rho_i(t)]$  decays exponentially  $n(t) = n(0)e^{-2\kappa t}$ , see the bottom inset in left main panel of Fig 3. This exponential growth leads to a regime beyond the validity of linearisation, which features underdamped relaxation oscillations of  $\psi(t)$ . Note that for the conservative case  $\kappa = 0$  this is replaced by undamped periodic oscillations<sup>32</sup>. At longer times,  $t\kappa > 1$ , the oscillations are damped out but the amplitude  $\psi(t)$  also decays to zero as  $\exp(-\kappa t)$  due to the photon loss. However, the field rescaled by the occupation,  $\bar{\psi}_i(t) = \psi_i(t)/\sqrt{n_i(t)}$  does reach a non-trivial steady state. This is shown in the top inset of Fig 3. In contrast, if one consid-

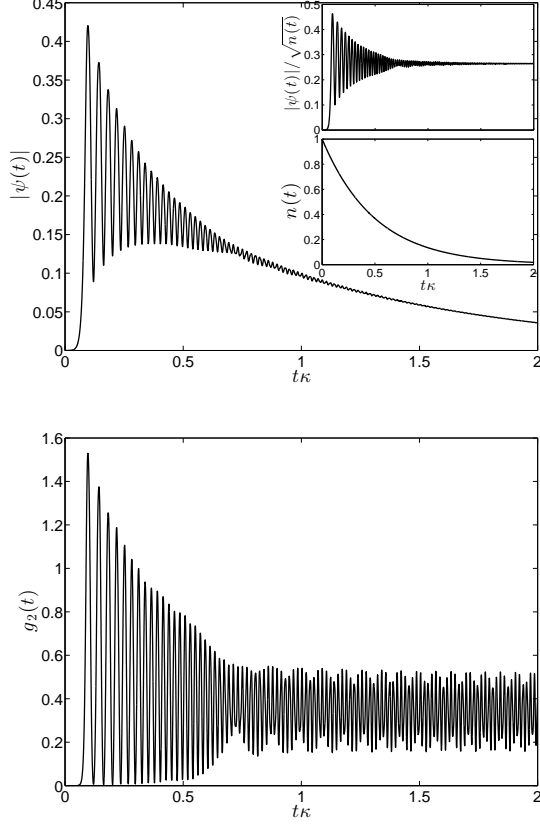


FIG. 3. Dynamics of a one-dimensional array ( $z = 2$ ) of  $N = 10$  coupled cavities in presence of a weak dissipation  $\kappa = 10^{-2}U$  and for  $zJ = 3U$ . Top panel: Time evolution of the absolute value of the order parameter  $|\psi(t)|$ . For the same parameters of the main panel, the bottom inset shows the evolution of the average filling  $\langle n \rangle = n(t)$ , while the top inset shows the rescaled order parameter  $\bar{\psi}(t) = |\psi(t)|/\sqrt{n(t)}$ . Bottom panel: Time evolution of the zero-time delay second order correlation function  $g_2(t)$ .

ered instead a case where  $J/U < J/U|_{\text{cr}}$  there would be no instability. One should however note that while the distinction between initial stability and instability depends only on the parameters of the model, the asymptotic value of  $\bar{\psi}(t)$  does depend (logarithmically) on the value of  $\eta$  chosen — for smaller  $\eta$  the instability takes longer to reach the nonlinear regime, and so the average photon number at this point is smaller, affecting the final state reached. Further information about the state can also be found from the correlation function  $g_2(t) = \text{Tr}[\hat{n}_i(\hat{n}_i - 1)\rho_i(t)]/n_i(t)^2$ . Again, because this quantity is normalized it asymptotically approaches a constant non-zero value (unless  $n_0 = 1$ ). One may in fact show that if  $J = 0$ ,  $g_2(t) = g_2(0) = 1 - 1/n_0$  remains fixed at the value determined by the initial Fock state.

Since the rescaled field  $\bar{\psi}(t)$  and correlation function  $g_2(t)$  approach asymptotic values at late times, the behaviour for a given set of initial conditions can be charac-

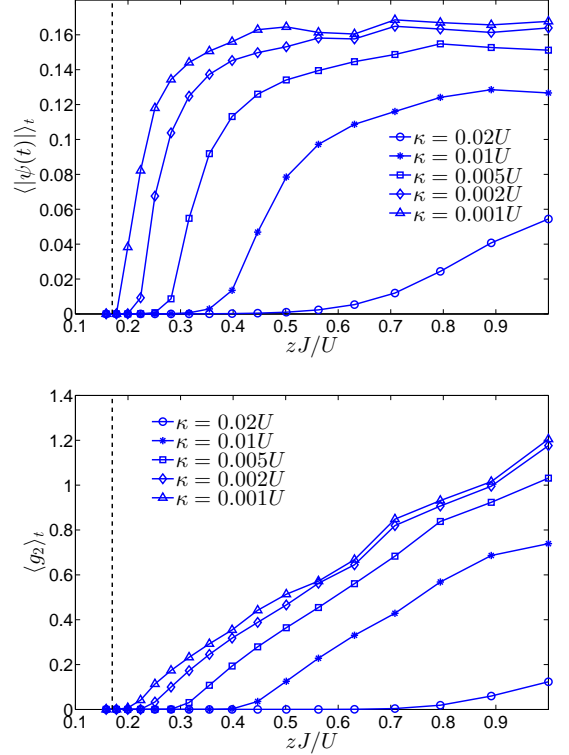


FIG. 4. Time average of  $|\psi(t)|$  (left panel) and  $g_2(t)$  (right panel) in the time interval  $1 < t\kappa < 2$  as a function of the hopping amplitude  $J/U$  for  $\kappa = 0.001U$  (triangles),  $\kappa = 0.002U$  (diamonds),  $\kappa = 0.005U$  (squares),  $\kappa = 0.01U$  (asterisks) and  $\kappa = 0.02U$  (circles). The vertical dashed line denotes the value at which the Mott insulator–superfluid transition occurs in the equilibrium Bose-Hubbard model at integer filling  $n_0 = 1$ ,  $zJ/U|_{\text{cr}} \approx 0.17$ .

terised by these values. Formally these are extracted by finding the time-averaged values  $\langle |\psi| \rangle_t$ ,  $\langle g_2 \rangle_t$ , averaging over a time window that neglects the initial transients as proposed by Tomadin *et al.*<sup>26</sup>. Such an approach is illustrated in Figure 4, which shows the time-averaged  $\langle |\psi| \rangle_t$  and  $\langle g_2 \rangle_t$  in the time interval  $1 < t\kappa < 2$ , as a function of the hopping amplitude  $J/U$  and for five different values of the photon decay rate  $\kappa$ . One may clearly see that below a threshold value of  $zJ/U$  both  $\langle |\psi| \rangle_t$  and  $\langle g_2 \rangle_t$  vanish. As  $\kappa \rightarrow 0$  this threshold approaches the equilibrium superfluid–insulator transition which occurs at  $zJ/U|_{\text{cr}} \approx 0.17$  for  $n_0 = 1$ . While these results occur in mean-field theory, similar results have been reported by using a cluster mean-field approach by Tomadin *et al.*<sup>26</sup>.

## B. Disordered case

We now explore the role played by the on-site cavity disorder  $\varepsilon_i$  in the non-equilibrium dynamics. As discussed above, we thus solve the Liouville problem Eq. (3)

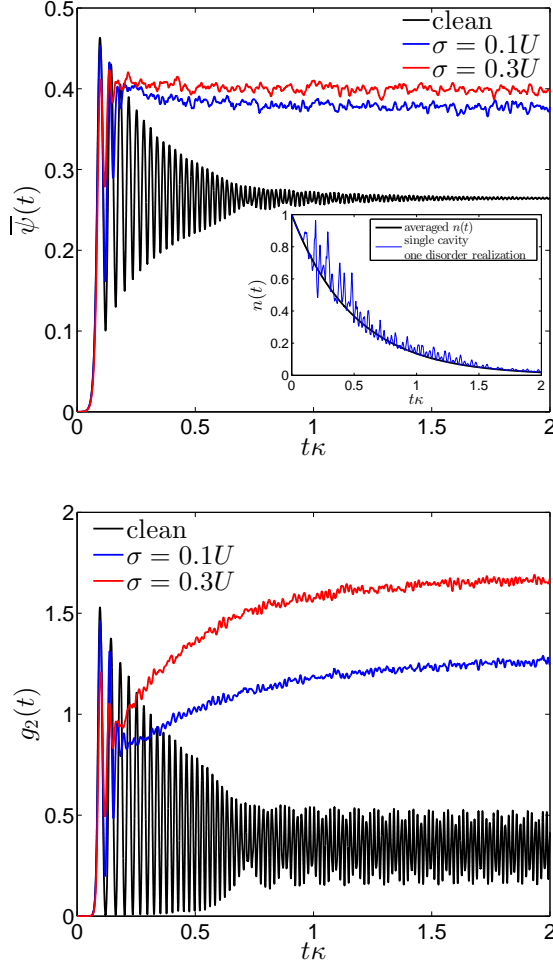


FIG. 5. Dynamics of a disordered one-dimensional array ( $z = 2$ ) consisting of  $N = 48$  coupled cavities in presence of a dissipation  $\kappa = 10^{-2}U$  and for  $zJ = 3U$ . The simulation has been performed for 10 different realisations of Gaussian distributed cavity energies with  $\sigma = 0.1U$  (blue line) and  $\sigma = 0.3U$  (red line). Top panel: Time evolution of the absolute value of the order parameter  $|\psi(t)|$ . The inset shows the evolution of the average filling  $\langle n \rangle = n(t)$  for a single cavity and a single realisation of disorder with  $\sigma = 0.1U$  (blue line) and after averaging over all the cavities and all the realisations (black line). Bottom panel: Time evolution of the zero-time delay second order correlation function  $g_2(t)$ .

drawing the cavity energies  $\varepsilon_i$  from a Gaussian distribution with standard deviation  $\sigma$ . In order to characterise the properties of the ensemble, rather than those specific to a particular realisation, we average the expectations  $|\psi|$  and  $g_2$  over different realisations of disorder, and additionally average over all sites within a given realisation.

Figure 5 shows the time evolution of both the order parameter (left panel) and the second-order correlation function (right panel) for a 1D array consisting of  $N = 48$  cavities, averaged over 10 realisations of the energies. Except for the distribution of site energies  $\varepsilon_i$ , all other pa-

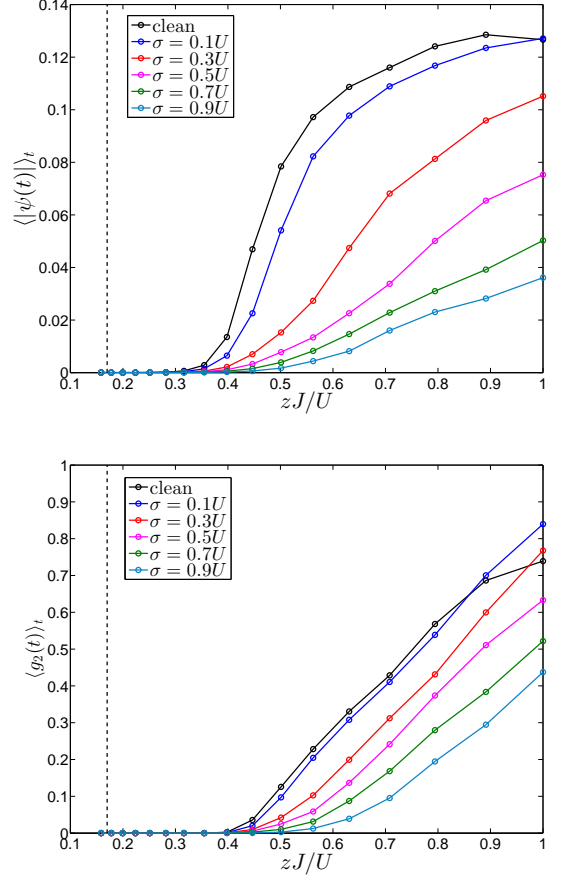


FIG. 6. Time average of  $|\psi(t)|$  (top panel) and  $g_2(t)$  (bottom panel) in the time interval  $1 < t\kappa < 2$  as a function of the hopping amplitude  $J/U$  for fixed decay  $\kappa = 0.01U$  and increasing disorder strength  $\sigma$ . The vertical dashed line identifies the value at which the Mott insulator-superfluid transition occurs in the equilibrium Bose-Hubbard model at integer filling  $n_0 = 1$ ,  $zJ/U|_{\text{cr}} \approx 0.17$ .

rameters are as in Fig. 3. The site energies are drawn from Gaussian distributions with  $\sigma = 0.1U$  (blue line) and  $0.3U$  (red line). At short times  $t\kappa < 0.1$ , the dynamics is characterised by the same linear instability as is seen in the clean case (black line), and both  $\psi(t)$  and  $g_2(t)$  increase exponentially. At later times however disorder strongly modifies the behaviour. The oscillations seen previously in the clean case are washed out by averaging over different cavities, and so a quasi-steady state value is reached earlier.

As in the clean case, the appearance of a plateau at late times suggests it is possible to characterise the evolution by its asymptotic value (see discussion in section IV). Figure 6 shows the time-integrated  $|\psi|$  (left panel) and  $g_2$  (right panel) as the ratio  $J/U$  is varied at a fixed photon dissipation constant  $\kappa = 10^{-2}U$  and for increasing values of disorder strength. As in the clean case, a threshold value of  $zJ/U$  is required before the instability



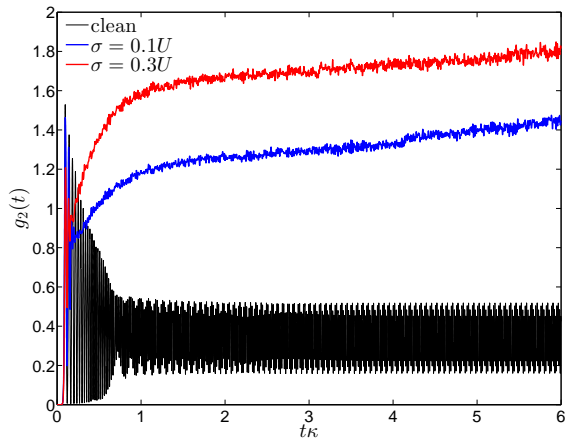


FIG. 7. Dynamics of a disordered one-dimensional array ( $z = 2$ ) consisting of  $N = 48$  coupled cavities in presence of a dissipation  $\kappa = 10^{-2}U$  and for  $zJ = 3U$ . The simulation has been performed for 10 different realisations of Gaussian distributed cavity energies with  $\sigma = 0.1U$  (blue line) and  $\sigma = 0.3U$  (red line).

occurs. This threshold value of  $zJ/U$  for the instability of the  $\psi = 0$  state appears to increase with increasing disorder. In equilibrium there is a “Bose glass” phase between the Mott insulator and the superfluid<sup>17</sup>, where particles are no longer localised by interactions, but are instead localised by disorder. The critical hopping  $zJ/U$  for the equilibrium transition between the Bose glass and superfluid phase increases with hopping, and so our observation of increasing critical  $zJ/U$ . The increasing critical  $zJ/U$  we observe for the threshold in the open system is consistent with this.

#### IV. RARE SITE STATISTICS AT LATE TIMES

While in the clean case, the plateau reached by  $\bar{\psi}(t)$  and  $g_2(t)$  around  $t\kappa \simeq 2$  reflects the asymptotic time dependence, this turns out not to be the case for the disordered lattice. Despite the appearance of an apparent plateau seen in figure 5 only indicates a temporary plateau. At later times, the values of  $\langle g_2(t) \rangle_{\text{dis}}$  starts to rise further as shown in figure 7. Intriguingly, this rise of  $\langle g_2(t) \rangle_{\text{dis}}$  at late times in fact reflects the existence of rare sites with large and exceptionally large values of  $g_2(t)$  which dominate the disorder average. This is illustrated in figure 8, which shows the probability density of  $g_2$  ( $P_{g_2}$ ) calculated for the same hopping and decay constants used in figure 7 using a sample of 2000 values of  $g_2$ , generated after the simulation of a 1D array of 100 cavities for 20 different realisations of disorder with  $\sigma = 0.3U$  (see the red curve in figure 7). The right panel shows that, at late times ( $t\kappa = 6$ ) some sites exhibit large values ( $> 5$ ) of  $g_2$ . This behaviour can be better understood by looking at figure 9, which illustrates for a

smaller hopping  $zJ = 0.5U$  and  $\kappa = 0.01U$ , how the disorder average  $\langle g_2(t) \rangle_{\text{dis}}$  rises when  $\sigma = 0.3U$  (see the red curve) as a result of the occurrence of rare sites with large values of  $g_2$ , as shown by the probability density evaluated at  $t\kappa = 1$  and  $t\kappa = 6$ , shown in figure 10. It is worth noticing that all the anomalous sites (i.e. with  $g_2 \gg 1$ ) are local minima of the potential (energy landscape), but not all the local minima exhibit such anomalous values of  $g_2$ . Further, following the evolution to much later times becomes difficult, as the large ratio between different elements of the density matrix introduces numerical errors.

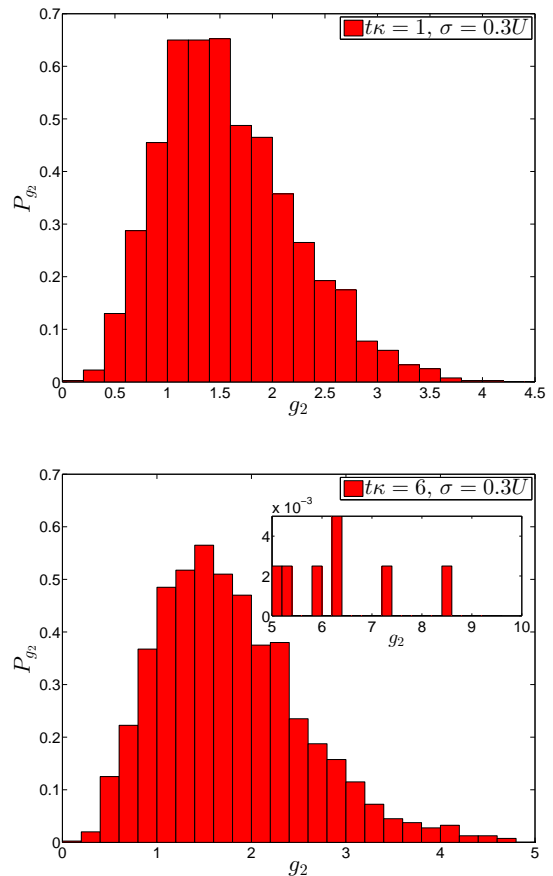


FIG. 8. Probability density of  $g_2$  calculated for a 1D array using  $\kappa = 0.01U$ ,  $zJ = 3U$  and  $\sigma = 0.3U$  (see the red curve in Fig. 7). The probability density has been evaluated using a sample of 2000 cavities, obtained simulating 20 different disorder realisations of an array consisting of 100 cavities. Top panel: the probability density of  $g_2$  at  $t\kappa = 1$ ; Bottom panel: the probability density of  $g_2$  at  $t\kappa = 6$ . The inset shows the occurrence of rare cavities with values of  $g_2$  larger than 5.

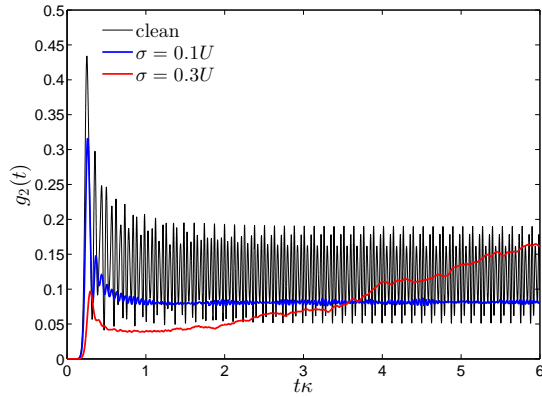


FIG. 9. Dynamics of a disordered one-dimensional array ( $z = 2$ ) consisting of  $N = 48$  coupled cavities in presence of a dissipation  $\kappa = 10^{-2}U$  and for  $zJ = 0.5U$ . The simulation has been performed for 10 different realisations of Gaussian distributed cavity energies with  $\sigma = 0.1U$  (blue line) and  $\sigma = 0.3U$  (red line).

## V. CONCLUSIONS

We have studied the time evolution of the disordered open Bose-Hubbard model following an initially prepared Mott state. As for the clean case, a dynamical transition does occur between small and large values of hopping, signalled by the asymptotic behaviour of the rescaled field  $\bar{\psi}(t)$ . We find that in line with the equilibrium expectations, the presence of disorder does increase  $zJ/U|_{\text{cr}}$ , i.e. does increase the hopping required for the superfluid instability to develop. However, even within mean-field theory, disorder can produce anomalous long time dynamics, where ensemble averages are dominated by the effect of rare sites.

## VI. ACKNOWLEDGEMENTS

We acknowledge financial support from an ICAM-I2CAM postdoctoral fellowship for the execution of this work. C.C. gratefully acknowledges support from ESF (Intelbiomat Programme), R.F. from IP-SIQS and PRIN (Project 2010LLKJBX), J.K. from EPSRC programme “TOPNES” (EP/I031014/1) and EPSRC

grant (EP/G004714/2), and H.E.T. from NSF CAREER (DMR-1151810) and The Eric and Wendy Schmidt Transformative Technology Fund. We acknowledge helpful discussions with Peter Littlewood.

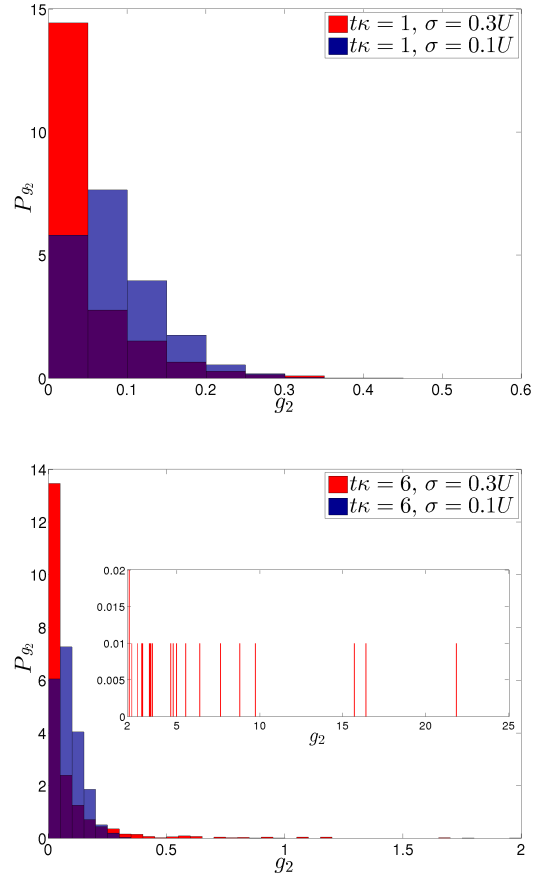


FIG. 10. Probability density of  $g_2$  calculated for a 1D array with  $\kappa = 0.01U$  and  $zJ = 0.5U$  as in Fig. 9. The probability density has been evaluated using a sample of 2000 cavities, obtained simulating 20 different disorder realisations of an array consisting of 100 cavities. Top panel: the probability density of  $g_2$  at  $t\kappa = 1$  for  $\sigma = 0.1U$  (blue) and  $\sigma = 0.3U$  (red); Bottom panel: the probability density of  $g_2$  at  $t\kappa = 6$ . The inset shows that when  $\sigma = 0.3U$  some cavities exhibit exceptionally large values of  $g_2$  up to  $\gtrsim 20$ .

<sup>1</sup> R. P. Feynman, Int. J. Theor. Phys. **2**, 527 (1982).

<sup>2</sup> E. Jané, G. Vidal, W. Dür, P. Zoller, and J. I. Cirac, Quantum Inf. and Comp. **3**, 15 (2003).

<sup>3</sup> I. Buluta and F. Nori, Science **326**, 108 (2009).

<sup>4</sup> A. A. Houck, H. E. Türeci, and J. Koch, Nature Physics **8**, 292 (2012).

<sup>5</sup> I. Bloch, J. Dalibard, and W. Zwerger, Rev. Mod. Phys. **80**, 885 (2008).

<sup>6</sup> C. Monroe and J. Kim, Science **339**, 1064 (2013).

<sup>7</sup> M. J. Hartmann, F. G. S. L. Brandão, and M. B. Plenio, Nature Physics **2**, 849 (2006).

<sup>8</sup> A. D. Greentree, C. Tahan, J. H. Cole, and L. C. L. Hollenberg, Nature Physics **2**, 856 (2006).

<sup>9</sup> D. Angelakis, M. Santos, and S. Bose, Phys. Rev. A **76**, 031805 (2007).

- <sup>10</sup> M. J. Hartmann, F. G. S. L. Brandão, and M. B. Plenio, *Laser & Photonics Reviews* **2**, 527 (2008).
- <sup>11</sup> A. Tomadin and R. Fazio, *Journal of the Optical Society of America B* **27**, A130 (2010).
- <sup>12</sup> A. Majumdar, A. Rundquist, M. Bajcsy, V. D. Dasika, S. R. Bank, and J. Vukovic, *Phys. Rev. B* **86**, 195312 (2012).
- <sup>13</sup> G. Lepert, E. A. Hinds, H. L. Rogers, J. C. Gates, and P. G. R. Smith, *Appl. Phys. Lett.* **103**, 111112 (2013).
- <sup>14</sup> D. L. Underwood, W. E. Shanks, J. Koch, and A. A. Houck, *Phys. Rev. A* **86**, 023837 (2012).
- <sup>15</sup> S. Schmidt and J. Koch, *Annalen der Physik* **525**, 395 (2013).
- <sup>16</sup> M. O. Scully and M. S. Zubairy, *Quantum Optics* (Cambridge University Press, Cambridge, 1997).
- <sup>17</sup> M. P. A. Fisher, P. B. Weichman, G. Grinstein, and D. S. Fisher, *Phys. Rev. B* **40**, 546 (1989).
- <sup>18</sup> T. Grujic, S. R. Clark, D. Jaksch, and D. G. Angelakis, *New Journal of Physics* **14**, 103025 (2012).
- <sup>19</sup> I. Carusotto, D. Gerace, H. E. Türeci, S. De Liberato, C. Ciuti, and A. Imamoglu, *Phys. Rev. Lett.* **103**, 033601 (2009).
- <sup>20</sup> M. J. Hartmann, *Phys. Rev. Lett.* **104**, 113601 (2010).
- <sup>21</sup> F. Nissen, S. Schmidt, M. Biondi, G. Blatter, H. E. Türeci, and J. Keeling, *Phys. Rev. Lett.* **108**, 233603 (2012).
- <sup>22</sup> J. Jin, D. Rossini, R. Fazio, M. Leib, and M. J. Hartmann, *Phys. Rev. Lett.* **110**, 163605 (2013).
- <sup>23</sup> G. Kulaitis, F. Krüger, F. Nissen, and J. Keeling, *Phys. Rev. A* **87**, 013840 (2013).
- <sup>24</sup> J. Werschnik and E. K. U. Gross, *Journal of Physics B: Atomic, Molecular and Optical Physics* **40**, R17 (2007).
- <sup>25</sup> R. T. Brierley, C. Creatore, P. B. Littlewood, and P. R. Eastham, *Phys. Rev. Lett.* **109**, 043002 (2012).
- <sup>26</sup> A. Tomadin, V. Giovannetti, R. Fazio, D. Gerace, I. Carusotto, H. E. Türeci, and A. Imamoglu, *Phys. Rev. A* **81**, 061801 (2010).
- <sup>27</sup> A. Polkovnikov, K. Sengupta, A. Silva, and M. Vengalattore, *Rev. Mod. Phys.* **83**, 863 (2011).
- <sup>28</sup> C. Kollath, A. M. Lauchli, and E. Altman, *Phys. Rev. Lett.* **98**, 180601 (2007).
- <sup>29</sup> B. Sciolla and G. Biroli, *Phys. Rev. Lett.* **105**, 220401 (2010).
- <sup>30</sup> M. Cheneau, P. Barmettler, D. Poletti, M. Endres, P. Schau, T. Fukuhara, C. Gross, I. Bloch, C. Kollath, and S. Kuhr, *Nature* **481**, 484 (2012).
- <sup>31</sup> A. Tomadin, *Dynamical instabilities in quantum many-body systems*, Ph.D. thesis, Scuola Normale Superiore, Pisa (2009).
- <sup>32</sup> E. Altman and A. Auerbach, *Phys. Rev. Lett.* **89**, 250404 (2002).
- <sup>33</sup> V. Gurarie, L. Pollet, N. V. Prokof'ev, B. V. Svistunov, and M. Troyer, *Phys. Rev. B* **80**, 214519 (2009).
- <sup>34</sup> U. Bissbort, R. Thomale, and W. Hofstetter, *Phys. Rev. A* **81**, 063643 (2010).
- <sup>35</sup> L. Pollet, "A review of monte carlo simulations for the Bose-Hubbard model" (2013), arXiv:1307.5430.